SI Appendix

Chloroplast SRP43 acts as a chaperone on glutamyl-tRNA reductase, the rate-limiting enzyme in tetrapyrrole biosynthesis

Peng Wang[a], Liang-Fu Cheng[b,1], Daniel Wittmann[a], Alex Siegel[b], Shu-ou Shan[b] and Bernhard Grimm[a,2]

[2] Correspondence may be addressed.

E-mail: bernhard.grimm@hu-berlin.de

This PDF file includes:

Materials and Methods

Plant materials and growth conditions. *Arabidopsis thaliana* mutant, including the maize transposon-containing null mutant for *cpSRP43* (*chaos*), the T-DNA insertion mutant lines for *cpSRP54* (*ffc*, CS850421), *cpftsy* (SALK_049077) and *gbp* (Salk_200203), and the *chaos/ffc* double mutant have been described previously (1, 2). The corresponding ecotypes Columbia-0 (Col-0, for *ffc*, *cpftsy*, and *gbp* mutants) and Landsberg-0 (Ler-0, for *chaos* mutant) were used as wild-type (WT) plants. The homozygous *chaos/gbp* double mutant was generated by crossing *chaos* as the female parent to the *gbp* mutant. Considering the genetic heterogeneity raised by the two *Arabidopsis* ecotypes, we used Col-0 and Ler-0 as controls for *chaos/gbp* double mutant. Furthermore, as GluTR level was specifically and pronouncedly decreased in the *chaos/gbp* double mutant, compared to *chaos/ffc*, which share the same genetic background (Figs. 1*B* and 2*B*), this observation cannot be attributed to potential ecotype polymorphism. *Arabidopsis thaliana* plants were grown in soil at 22 °C and 70% humidity on a 16-h photoperiod (120 μmol photons m^{-2} s^{-1}). Three- to four-week-old plants were analyzed.

To generate *chaos* mutant complementation lines, a full-length cDNA, derived from *cpSRP43* (AT2G47450) and encoding cpSRP43 including its transit peptide, was amplified from Arabidopsis total Col-0 cDNA using the primer pair pGL1-cpSRP43 (Table S1). This fragment was cloned into pJet1.2 (Thermo Scientific) and used for site-directed mutagenesis of specific domains in cpSRP43 by overlapping PCR using primer pairs listed in Table S1. The wild-type *cpSRP43* sequence and truncated cpSRP43 coding sequences lacking one or other of the four encoded domains in cpSRP43 (Fig. 5*A*) were cloned into the binary vector pGL1 (3), in which gene expression is driven by the CaMV 35S promoter. Homozygous *chaos* mutants were transformed with each of these pGL1 derivatives using the *Agrobacterium tumefaciens* strain GV2260. Transgenic plants were selected by screening for resistance to the herbicide BASTA. F3 homozygous transgenic lines were used in this study.

Nucleic acid analysis. Arabidopsis genomic DNA was isolated as described previously (4). The maize transposon insertions in the *chaos* mutant and in the various *chaos* complementation lines were recovered by PCR using combinations of transposon- and gene-specific primers [Fig. S6 and Table S1(5)].

Total RNA was extracted from Arabidopsis leaf material frozen in liquid nitrogen using TRIsure (Bioline) according to the manufacturer's protocol. For each RNA sample, a pool of at least three individual plants was harvested. For each biological repeat, at least three RNA samples were prepared for each wild-type, mutant, or transgenic line. Aliquots (2 μg) of DNase-treated RNA were primed with oligo(dT) and reverse transcribed into cDNA using RevertAid reverse transcriptase (Thermo Fisher Scientific). Expression of genes encoding cpSRP43, TBS enzymes and regulators was determined by quantitative real-time PCR. The qRT-PCR was performed with 2×qPCR mastermix (BioTool) using an IQ5 multicolor real-time PCR detection system (Bio-Rad). *ACTIN2* (AT3G18780) and *SAND* (AT2G28390) were routinely used as reference genes. The qRT-PCR primers are listed in Supplemental Table 1. Calculation of relative gene expression was done with the Biorad CFX-manager software (1.6) and is given as $2^{-\Delta\Delta Ct}$.

HPLC analysis of tetrapyrroles. Photosynthetic pigments and Chl precursors were extracted from homogenized Arabidopsis leaf materials using acetone:0.2 M NH_4OH (9:1, v/v). After centrifugation (20,000*g*,

20 min, 4°C), the supernatant was collected for HPLC analysis. The non-covalently bound heme was extracted from the pellet by incubation in acetone:hydrochloric acid:dimethylsulfoxide (10:0.5:2, v/v/v). The HPLC analysis was performed using reversed-phase chromatography on Agilent HPLC systems as described previously (6).

Determination of ALA synthesis rate. ALA-synthesizing capacity was determined as described previously (7). Briefly, about 30-mg samples of detached leaves from 3-week-old plants were incubated in 5 mL of 50 mM Tris-HCl (pH 7.2) containing 40 mM levulinic acid (Sigma-Aldrich) for 3 h under growth light conditions, and then homogenized in liquid nitrogen. Frozen leaf material was resuspended in 0.5 mL of 20 mM potassium phosphate buffer (pH 7.2). After centrifugation (12,000 *g*, 5 min, 4 °C), 0.4 mL of leaf homogenate was mixed with 0.1 mL of ethyl acetoacetate (Sigma-Aldrich) and boiled for 10 min at 100 °C. Chilled samples were mixed with 0.5 mL of Ehrlich's reagent (373 mL of acetic acid, 90 mL of 70% [v/v] perchloric acid, 1.55 g of $HgCl_2$, 9.10 g of 4-dimethylamino benzaldehyde, and 500 mL of double distilled water) and centrifuged for 5 min at 12,000*g* at 4 °C. The absorption of the ALA pyrrole was measured at 525, 553, and 600 nm. The ALA content was calculated using a dilution curve constructed with an authentic ALA solution (Sigma) and was normalized with respect to the incubation time and fresh weight of leaf material used.

Bimolecular fluorescence complementation (BiFC) assay. The BiFC assay was performed as described before (2, 8, 9). The full-length cDNA fragments (with the encoded transit peptide) coding for cpSRP43 and cpSRP54 were cloned either into the pSPYNE (to produce fusion proteins containing the N-terminal part of YFP, nYFP) or pSPYCE (to fuse each to the C-terminal part of YFP, cYFP), whereas the full-length coding sequences of GluTR, GluTRΔHBD, GluTR-$N_{64\text{-}163}$, GluTRΔFBD, GBP, FLU, ALAD, and CHLM were each cloned into the pSPYCE vector only. The BiFC constructs were transiently transformed into the lower epidermal cells of *Nicotiana benthamiana* leaves using *Agrobacterium tumefaciens* strain GV2260. Infiltrated plants were then grown in darkness for 72 h before leaf segments from infiltrated areas were analyzed for reconstitution of YFP fluorescence using a confocal laser-scanning microscope (Leica TCS SP2; excitation at 514 nm, YFP emission 530 to 555 nm, Chl emission 600 to 700 nm).

Expression and purification of recombinant proteins. A cDNA fragment encoding the mature cpSRP43 protein was cloned into the pET28a expression vector using primers listed in Table S1. The pQE80L-GluTR, pQE80L-GluTRΔHBD, and pQE80L-GBP vectors for expression of N-terminal His-tagged proteins were reported previously (9). For large-scale expression and purification of His-tagged proteins, the *E. coli* expression vectors were transformed into the BL21 (DE3) strain, which was cultured in 2×YT medium. The bacterial culture was inoculated with $1/100^{th}$ of an overnight culture, and grown for 2.5 to 3 h at 37°C to an optical density of 0.4 to 0.6 (absorbance at 600 nm). The expression of recombinant proteins was then induced by adding 0.4 mM isopropylthio-β-galactoside for 3 h at 30 °C. *E. coli* cells were harvested, immediately frozen in liquid nitrogen, and stored at -80 °C until the pellets were used for purification. All His-tagged proteins were purified under native conditions according to the QIAexpressionist protocol (Qiagen) using Ni-NTA agarose, concentrated (with buffer exchange) by passage through Amicon Ultra-4 Centrifugal Filter Units (Merck-Millipore), then aliquoted and stored at -80 °C in 1×PBS containing 5% (v/v) glycerol.

The plasmids encoding GluTRΔHBD and the loop1-TM2-L18 fragment of LHCb5 were constructed using the QuikChange procedure (Stratagene). The plasmid used to express His_6-SUMO-GBP was created by Gibson assembly.

Wild-type and mutant LHCb5, GST, cpSRP43 and GST-cpSRP43 were overexpressed and purified as previously described (2, 10). GluTR and GBP were overexpressed and purified as previously described (2) with the following modifications. His_6-GluTR was overexpressed in NiCO21 (DE3) cells and affinity-purified on nickel-nitrilotriacetic acid (Ni-NTA) resin (Qiagen) followed by a negative purification using Chitin (NEB) resins. The partially purified GluTR was then applied to a MonoQ column (GE Healthcare) and eluted using a gradient of 100–350 mM NaCl. ΔHis-GBP was directly eluted from Ni-NTA by SUMO protease treatment of His_6-SUMO-GBP, and the resulting protein was further purified by elution from a MonoQ column using a gradient of 110 –230 mM NaCl.

The 54M peptide (QKAPPGTARRKRKAC) was custom synthesized by Eton Bioscience (99% purity), and the HBD peptide (ASSDSASNAASISALEQLKNSAADRYTKERC) was custom synthesized by GenScript (98% purity). The L18 peptide (VDPLYPGGSFDPLGLADD) was custom synthesized by AnaSpec (>95% purity). The HBD peptide (50 μM) was treated with 10 mM Tris(2-carboxyethyl)phosphine (TCEP) overnight at room temperature and labeled with 2 mM fluorescein-maleimide (Invitrogen) for 4 h at room temperature. The labeled peptide was purified by reversed-phase HPLC to remove the free dye. To generate a fluorescently labeled substrate for cpSRP43, a mutant version (G162C) of the loop1-TM2-L18 fragment of LHCb5 (50 μM), was incubated with fluorescein-maleimide (1.5 mM) for 4 h at room temperature under denaturing conditions (8 M urea, 20 mM K-HEPES, pH 7.5, 5 mM EDTA) to attach the fluorescent moiety to the Cys residue. Labeled protein was purified through Sephadex G25 to remove the free dye.

In vitro and in vivo pull-down analysis. In vitro His pull-down analysis was performed as described previously (2) with the following modifications. Purified His-GluTR and His-GluTRΔHBD proteins were used as baits, and incubated with purified GST, GST-cpSRP43, and ΔHis-GBP proteins, at 25 °C for 2 h. Then 50 μl of an equilibrated 50% (v/v) slurry of Ni-NTA agarose (Thermo Fisher Scientific) was added to each tube and incubated for 1 h at 80 rpm at 4 °C. The Ni-NTA agarose was collected by centrifugation (3,000 rpm, 3 min, 4 °C), and washed three to four times using binding buffer containing 20 mM imidazole. Finally, His-tagged proteins and their potential interaction proteins were eluted with binding buffer containing 300 mM imidazole. The eluted proteins were denatured in 2×Laemmli sample buffer and separated on a 12% SDS-PA gel. The potential interacting partners of cpSRP43 were detected by silver staining or immunoblot analysis.

In vivo His pull-down analysis was performed as described previously(11) with the following modifications. Purified His-cpSRP43 proteins (50 μg) were used as bait, and incubated with total chloroplast extracts (100 μg of Chl), which had been solubilized with 1% (w/v) dodecyl maltoside (DM) in binding buffer (25 mM Tris-HCl [pH 7.8], 150 mM NaCl, 5 mM $MgCl_2$, 10% [v/v], glycerol, and cOmplete protease inhibitor [Roche]) overnight at 4 °C. Solubilized total chloroplast extracts that had not been incubated with His-cpSRP43 were used as a negative control. An aliquot (50 μl) of an equilibrated 50% (v/v) slurry of Ni-NTA agarose (ThermoFisher Scientific) was then added to each tube and incubated for 1 h at 80 rpm at 4 °C. All subsequent steps were carried out as described above.

In vivo immunoprecipitation analysis was carried out as described previously (12) with some modifications. Intact chloroplasts (100 µg of Chl) isolated from transgenic plants expressing cpSRP43-FLAG or from wild-type (Col-0) plants (used as negative control) were solubilized in binding buffer containing 1% (w/v) DM, 25 mM Tris-HCl (pH 7.8), 150 mM NaCl, 5 mM $MgCl_2$, 10% (v/v), glycerol, and cOmplete protease inhibitor (Roche) for 5 min on ice. After centrifugation (15,000 rpm, 10 min, 4 °C), the supernatant was incubated overnight at 80 rpm and 4 °C with 10 µl of anti-FLAG antibody-conjugated agarose beads (Biotool) suspended in binding buffer. The beads were then pelleted by centrifugation (5,000 rpm, 30 sec, 4°C) and washed three to five times with binding buffer without DM to release the bound FLAG-cpSRP43 proteins and their interaction partners. Finally, the supernatant containing the FLAG-tagged cpSRP43 and its interaction partners was added to 2×Laemmli sample buffer and heated prior to SDS-PAGE. The potential interaction partners of cpSRP43-FLAG were detected by immunoblot analysis.

Fluorescence anisotropy measurements. All measurements were carried out at 25 °C in buffer D (50 mM HEPES, pH 7.5, 200 mM NaCl) on Fluorolog 3-22 (Yobin Yvon). The samples were excited at 495 nm, and fluorescence anisotropy values were recorded at 520 nm.

To measure the interaction of loop1-TM2-L18 with cpSRP43, varying concentrations of cpSRP43 were added to fluorescein-labeled loop1-TM2-L18 (100 nM). The fluorescence data were fitted to Eq. 1,

$$A_{obsd} = A_0 + \Delta A \frac{[S] + [pro] + K_d - \sqrt{([S] + [pro] + K_d)^2 - 4[S][pro]}}{2[S]} \qquad \text{(Eq. 1)}$$

in which A_{obsd} is the observed anisotropy value, A_0 the anisotropy value without cpSRP43, ΔA the change in anisotropy at saturating cpSRP43 concentrations, [S] the molar concentration of the substrate (loop1-TM2-L18), [pro] the concentration of the titrant, and K_d the equilibrium dissociation constant for the interaction of cpSRP43 with loop1-TM2-L18.

To verify competition between loop1-TM2-L18 and the L18 peptide for binding to cpSRP43, fluorescein-labeled loop1-TM2-L18 (100 nM) was pre-incubated with 400 nM cpSRP43 for 5 min as before and the preformed complex was challenged with increasing concentrations of unlabeled L18 peptide. Anisotropy values were recorded at equilibrium and plotted as a function of [L18]. The data were fitted to Eq. 2,

$$A_{obsd} = A_0 - \Delta A \frac{[L18]}{[L18] + K_i^{app}} \qquad \text{(Eq. 2)}$$

in which A_{obsd} is the observed anisotropy value, A_0 is the anisotropy value in the absence of L18, ΔA is the change in anisotropy at saturating L18 concentrations, and K_i^{app} is the apparent inhibition constant.

To detect binding of GluTR to substrate-bound cpSRP43, loop1-TM2-L18-fluorescein was pre-incubated with cpSRP43 (full-length or SBD) for 5 min as described above, and increasing concentrations of wild-type or mutant GluTR were added to the preformed complex. Fluorescence anisotropy values were recorded at equilibrium and plotted as a function of GluTR concentration. The data were fit to Eq 1.

Isolation of intact chloroplast and total thylakoid membranes. Chloroplast isolation was performed as described previously (13) with the following modifications. Briefly, 3-week-old Arabidopsis plants were homogenized in isolation buffer (0.33 M sorbitol, 20 mM HEPES-KOH pH 8.0, 5 mM $MgCl_2$, 5 mM EDTA, 5 mM EGTA, and 10 mM $NaHCO_3$), filtered through one layer of Miracloth (Calbiochem) and centrifuged for 5 min at 1,000*g*. The pellets were gently resuspended, loaded onto two-step Percoll gradients (40% and 80% in

isolation buffer), and centrifuged for 15 min at 6,500*g*. Chloroplasts were collected from the interface between the Percoll suspensions and washed twice with HMS buffer (0.3 M sorbitol, 50 mM HEPES-KOH pH 8.0, 5 mM $MgSO_4$). Thylakoid membranes were isolated from 3-week-old plants as described previously (14). The chloroplasts or thylakoid membranes were either used directly or frozen in liquid nitrogen.

Two-dimensional BN-SDS-PAGE. BN-PAGE was performed as described previously (14). Excised BN-PAGE lanes were then treated in SDS sample buffer (50 mM Tris-HCl, pH 6.8, 2% [w/v] SDS, 10% glycerol,0.002% [w/v] bromophenol blue, and 50 mM DTT) for 1 h at room temperature and loaded onto 11% SDS-PA gels containing 6 M urea to dissociate the individual complexes and separate their components. After electrophoresis, the SDS-PA gels were stained with Coomassie Brilliant Blue G250.

Protein extraction and immunoblot analysis. Total leaf and total thylakoid proteins were extracted from frozen leaf material or freshly isolated thylakoid membranes, respectively, according to (1, 2). Protein concentration was determined using the BCA kit (Thermo Fisher Scientific). For immunoblot analysis, equal amounts (15 µg) of plant proteins were fractionated on 12% SDS-PA gels, transferred to nitrocellulose membranes (GE Healthcare), and probed with specific antibodies. Antibodies against GluTR, GBP, FLU, GSAAT, ClpS, CHLM, and CHLP were generated in our lab (2, 3, 9), those for CHL27, YCF54, POR, D1, CP43, CP47, PsaA, PsaH, PsaL, Cyt f, ATPase β, LHCa1, and LHCb1 were purchased from Agrisera, and those for GFP, FLAG, and c-Myc were obtained from Sigma-Aldrich. The anti-CHLI antibody was kindly provided by Prof. Meizhong Luo (Huazhong Agricultural University, Wuhan, China). The antibodies against cpSRP43, cpSRP54, cpFtsY, and ALB3 were kindly donated by Prof. Danja Schünemann (Ruhr University Bochum, Germany). Immunoblot signals were detected with the SuperSignal West Pico Chemiluminescent Substrate (ThermoFisher Scientific).

Light scattering assay. The light scattering assay was performed as described previously (10, 15, 16). For formation of aggregates, unfolded GluTR fragments dissolved in 8 M urea were directly diluted into buffer D (50 mM HEPES, pH 7.5, 200 mM NaCl) containing varying concentrations of cpSRP43. Light scattering was monitored at 360 nm until equilibrium was reached. The percentage of soluble GluTR-N (% soluble) at equilibrium was plotted as a function of cpSRP43 concentration. The data were fitted to Eq. 3,

$$\%\ \text{soluble} = \Delta A \frac{[S] + [pro] + K_d - \sqrt{([S] + [pro] + K_d)^2 - 4[S][pro]}}{2[S]} \qquad \text{(Eq. 3)}$$

in which [pro] is molar concentration of cpSRP43, ΔA the % soluble at saturating cpSRP43 concentrations, [S] the molar substrate (GluTR-N) concentration, and K_d the equilibrium dissociation constant for the interaction of cpSRP43 with GluTR-N.

Sedimentation assay. The sedimentation assay was performed as described previously (10, 16). Unfolded GluTR fragments was diluted to 10 µM in Buffer D in the presence or absence of recombinant cpSRP43 protein, and incubated at 25 °C for 5 min. The mixtures were centrifuged at 16,000*g* for 30 min, and soluble and pellet fractions were denatured by boiling, fractionated and visualized by SDS-PAGE.

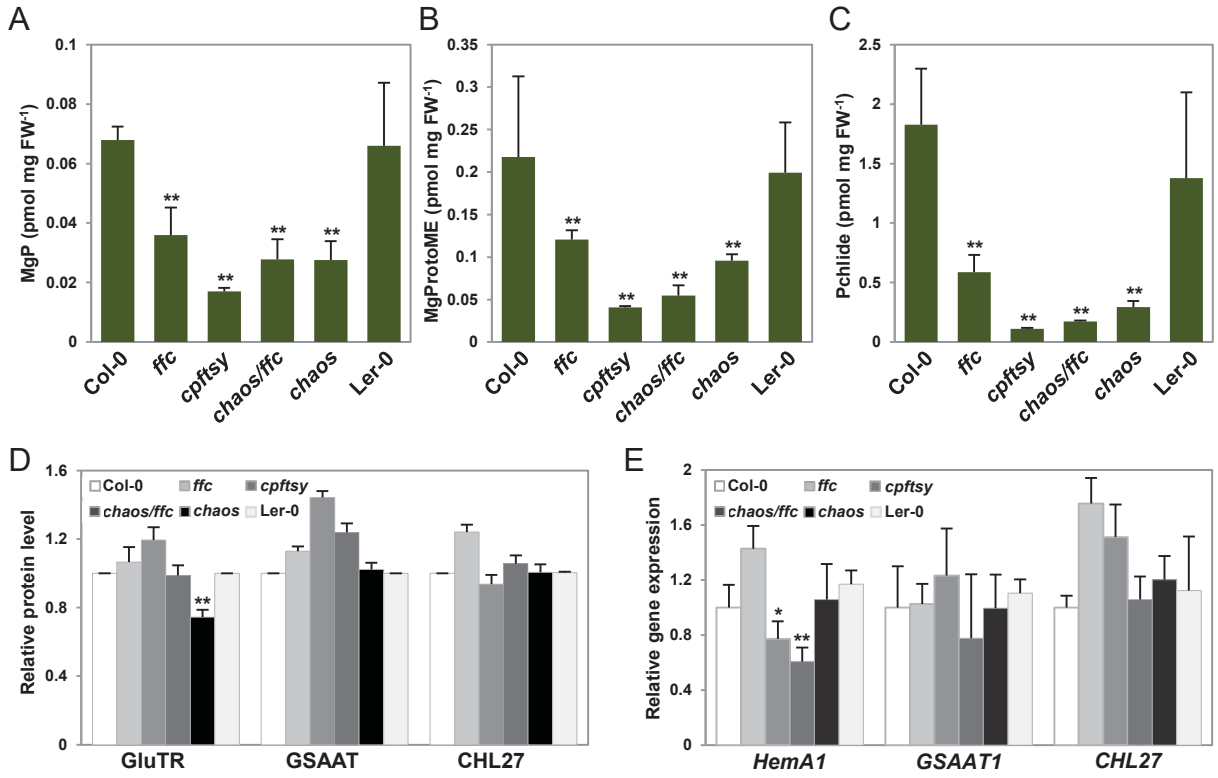

Fig. S1. Characterization of TBS in *cpsrp* mutants. (*A*-*C*) Accumulation of Chl precursors: Mg protoporphyrin (MgP, *A*), MgProto monomethylester (MgProtoME, *B*) and protochlorophyllide (Pchlide, *C*) in wild-type (WT, Col-0 and Ler-0) and *cpsrp* seedlings. (*D*) Semiquantitative analysis carried out with Phoretix 1D software (Phoretix International) of immunoblots in Fig. 1*D* from two biological replicates. Protein levels in *ffc* and *cpftsy* are shown relative to those in the corresponding wild-type ecotype Col-0 (1), while data for *chaos* and *chaos/ffc* are shown relative to the level in the wild-type ecotype Ler-0 (1). (*E*). Relative gene expression in WT and *cpsrp* mutants. *HEMA1* encodes the predominant isoform of GluTR in photosynthetic tissues. In *A*-*E*, data are means of three replicates ± SD. Asterisks indicate significant differences compared with the wild-type plants (*$P < 0.05$, **$P < 0.01$, Student's *t* test).

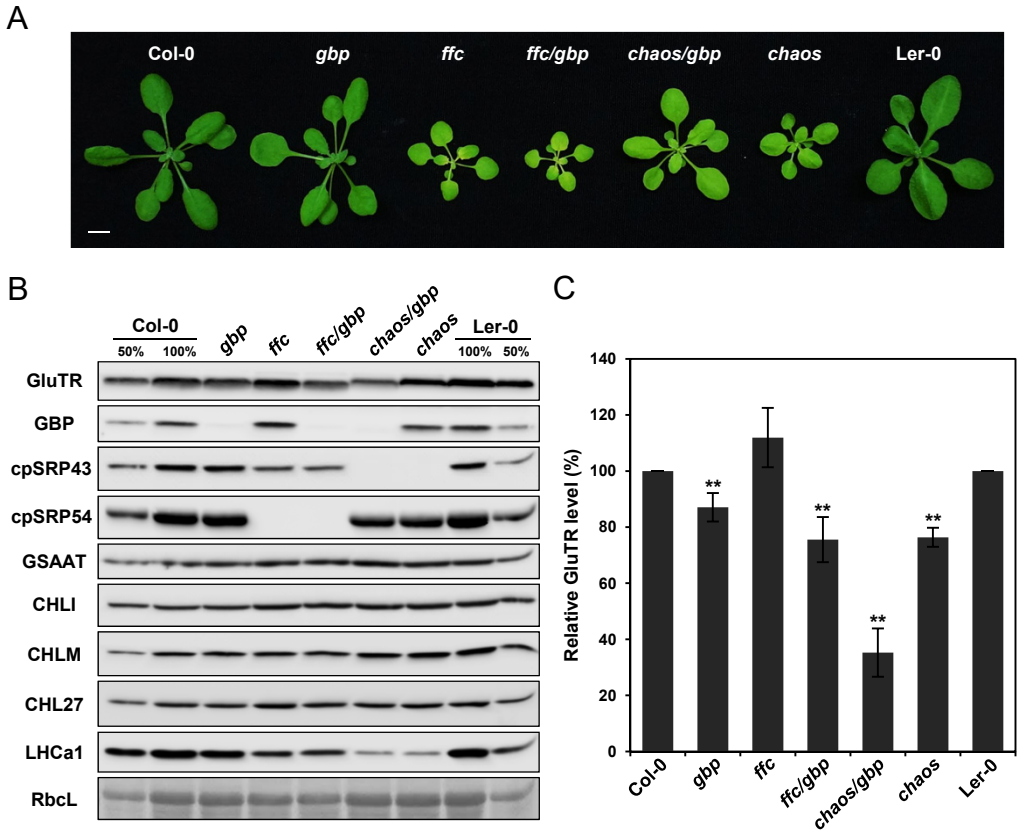

Fig. S2. Characterization of *chaos/gbp* and *ffc/gbp* double mutants. (*A*) Pale-green leaf phenotype of 28-day-old wild-type (Col-0 and Ler-0), *gbp*, *ffc*, *chaos*, *ffc/gbp* and *chaos/gbp* mutants. (Scale bars: 1 cm.) (*B*) Steady-state protein levels of TBS proteins, cpSRP components, and LHC proteins in seedlings were detected by immunoblotting using the indicated antibodies. The Ponceau S-stained RbcL is shown as a loading control. (*C*) Semiquantitative analysis of immunoblots in Fig. 2*B* and Fig. S2*B* from three biological replicates by using Phoretix 1D software (Phoretix International). The relative protein levels in *gbp*, *ffc*, and *ffc/gbp* mutants are shown relative to the level in Col-0. In contrast, the protein levels in *chaos* and *chaos/gbp* mutants are shown relative to the level in Ler-0. Data are means ± SD (n = 3). Asterisks indicate significant differences compared with the wild-type plants (*P < 0.05, **P < 0.01, Student's t test).

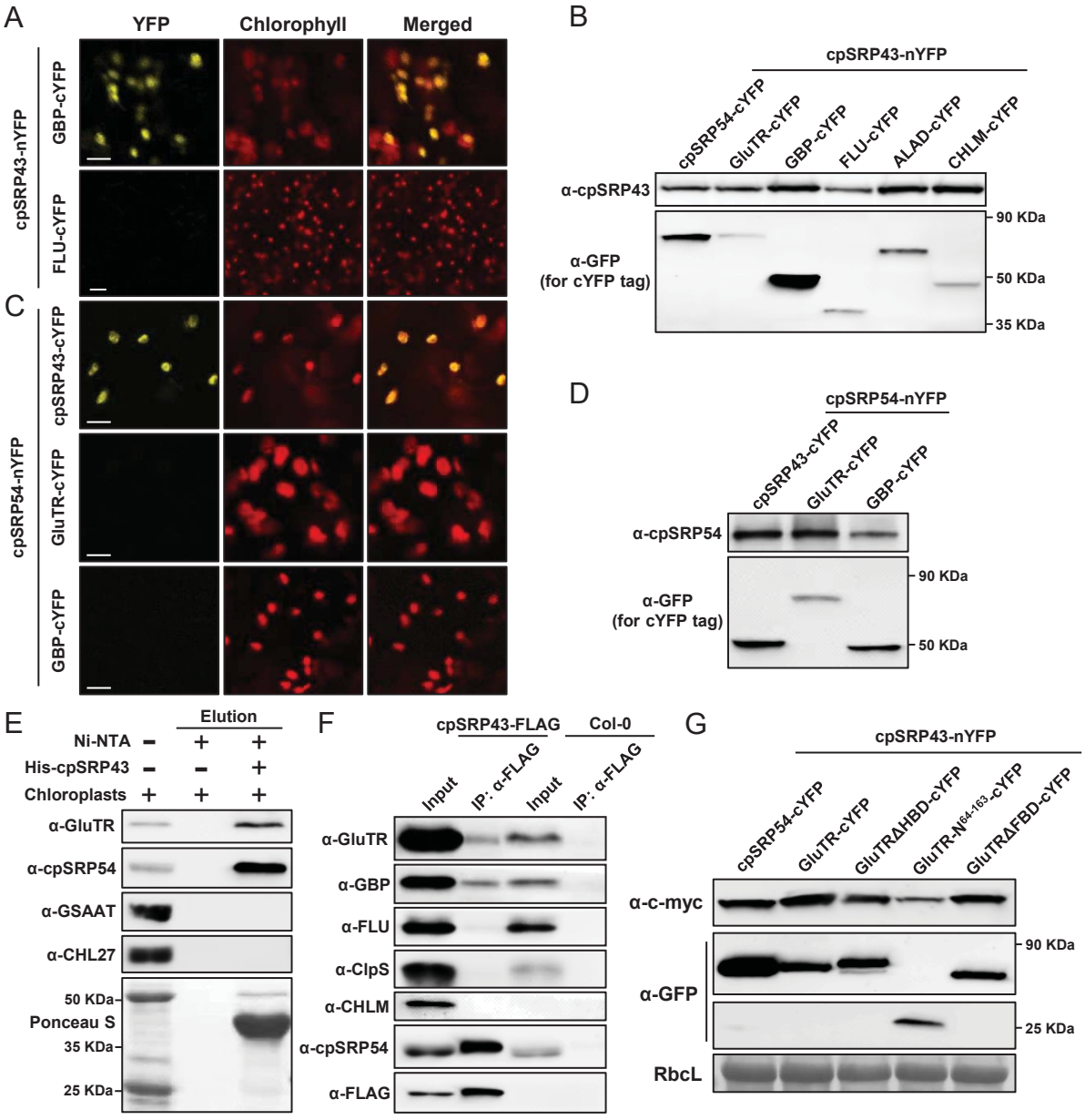

Fig. S3. Protein-protein interaction between cpSRP components and TBS proteins. (*A*) BiFC assays show interaction between cpSRP43 and two GluTR regulators, GBP and FLU. The cpSRP43 protein was fused to the N-terminal half of YFP, and GBP or FLU to its C-terminal half, and expressed in *N. benthamiana* following Agrobacterium infiltration. FLU was used as a negative control. (Scale bars: 10 μm.) (*B*) Immunoblotting analyses confirmed expression of cpSRP43-nYFP (with cpSRP43 antibody) and cpSRP54-/GluTR-/GBP-/FLU-/ALAD-/CHLM-cYFP (with GFP antibody) in Fig. 3*A* and Fig. S3*A*. (*C*) BiFC analysis of interaction between cpSRP54 and GluTR/GBP. CpSRP54 fused to the N-terminal half of YFP and cpSRP43, GluTR, or GBP fused to the C-terminal half of YFP, was expressed in *N. benthamiana* as described above. CpSRP43 was used as a positive control. (Scale bars: 10 μm.) (*D*) Immunoblotting analyses confirmed expression of cpSRP54-nYFP (cpSRP54 antibody) and cpSRP43-, GluTR-, and GBP-cYFP (GFP antibody) in Fig. S3*C*. (*E*) In vivo pull-down assay. Purified recombinant purified His-cpSRP43 was used as bait and incubated with total chloroplast extracts. Proteins bound to cpSRP43 were eluted with elution buffer containing 300 mM imidazole and detected by immunoblotting using the indicated antibodies. The total chloroplast extract and elution fractions were visualized by staining of nitrocellulose membranes with Ponceau S. (*F*) In vivo immunoprecipitation assay. Total chloroplast extracts from *Arabidopsis* transgenic plants overexpressing *cpSRP43-FLAG* (cpSRP43-FLAG) and wild-type plants (Col-0, used as negative control) were incubated with the anti-FLAG affinity gel (Sigma), and cpSRP43 interaction partners were then recovered by centrifugation, and identified by immunoblotting using the indicated antibodies. In *E* and *F*, cpSRP54 was used as positive control, whereas TBS proteins, such as FLU, GSAAT, CHLM, and CHL27, and ClpS were used as negative controls. (*G*) Immunoblotting analyses of protein extracts after the BiFC assay (shown in Fig. 6*B*) confirmed expression of cpSRP43-nYFP (c-Myc antibody) and cpSRP43 and GluTR variants containing cYFP (GFP antibody).

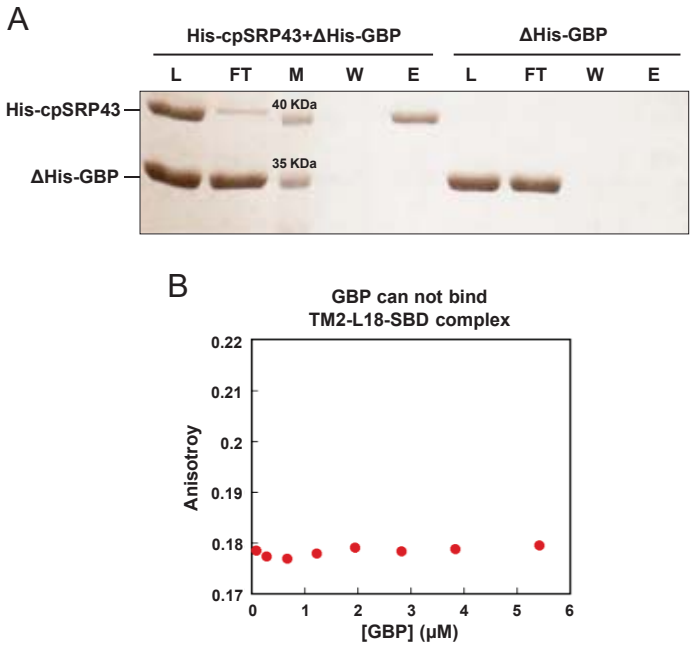

Fig. S4. GBP does not bind directly to cpSRP43. (*A*) In vitro pull-down assay based on His-tagged cpSRP43. Purified recombinant His-cpSRP43 (5 μM) was used as bait and incubated with 10 μM ΔHis-GBP. The proteins bound to His-cpSRP43 were eluted with elution buffer containing 200 mM imidazole. The loading control (L), flow-through (FT), protein molecular weight marker (M), wash (W) and elution (E) fractions were subjected to SDS-PAGE and stained with Coomassie Blue. ΔHis-GBP that had not been incubated with His-cpSRP43 was used as a negative control. (*B*) GBP does not alter the fluorescence anisotropy of the fluorescein-labeled LHCb5 fragment pre-bound to cpSRP43.

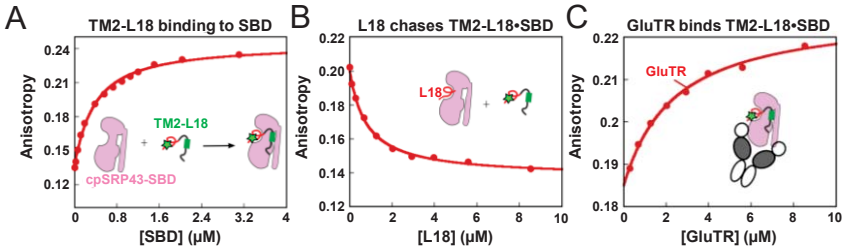

Fig. S5. The SBD of cpSRP43 interacts with GluTR. (*A*) Binding of the loop1-TM2-L18 fragment of LHCb5 to the SBD was measured by changes in fluorescence anisotropy. The data were fit to Eq. 1 and yielded a K_d value of 332 nM. Observed effect of the L18 peptide (*B*) or His-GluTR (*C*) on the fluorescence anisotropy of the LHCb5 fragment pre-bound to SBD. The data in (*B*) were fit to the competition model described by Eq. 2 and gave a value of 0.8 mM. The data in (*C*) were fit to Eq. 1 and gave a K_d value of 2.3 μM for GluTR. The SDs for the K_d and values were estimated to be ±10% based on at least two measurements each.

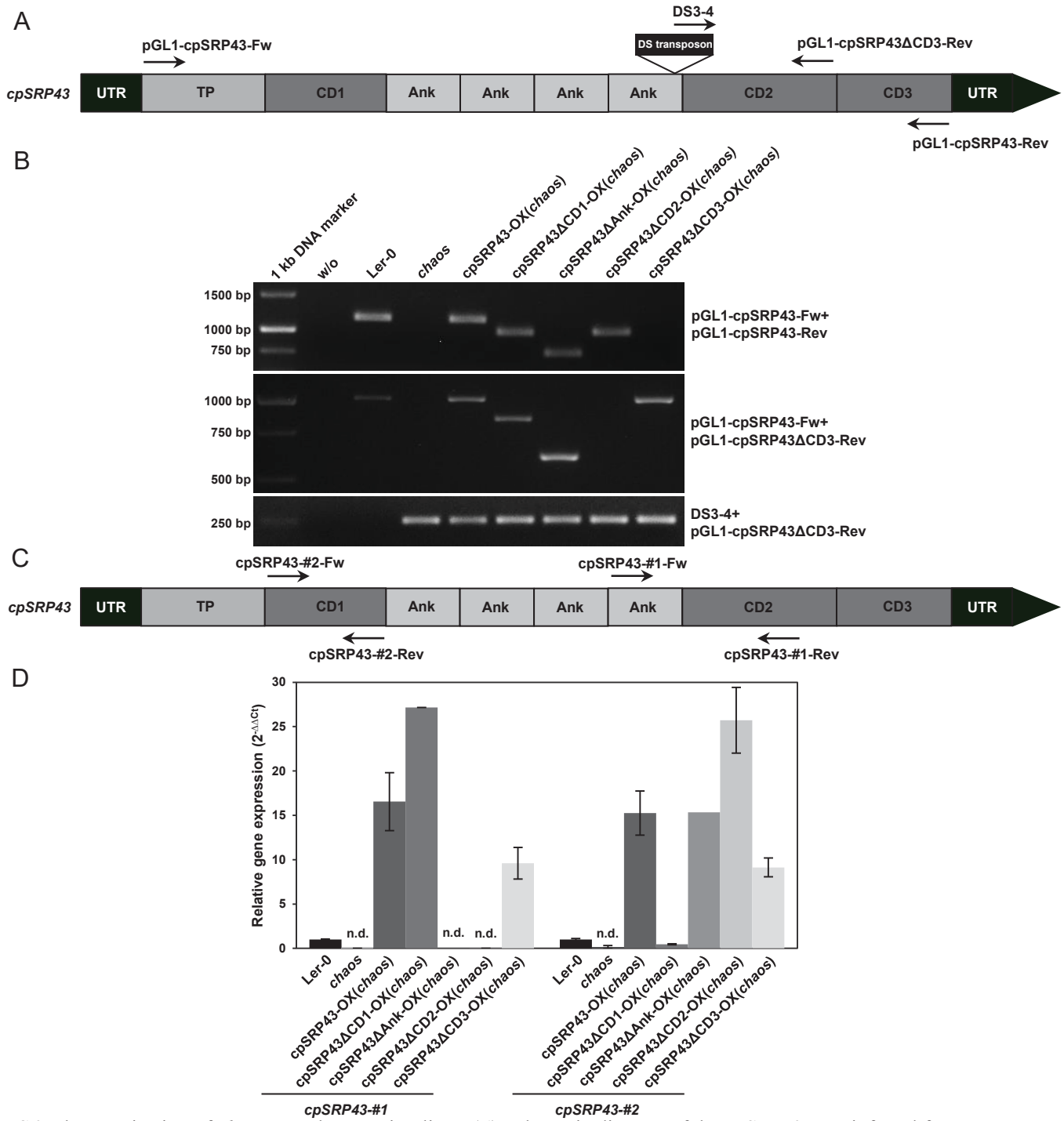

Fig. S6. Characterization of *chaos* complementation lines. (*A*) Schematic diagram of the *cpSRP43* gene inferred from DNA sequence analysis. The 5' and 3' untranslated regions (UTR, in black) and the various segments encoding cpSRP43 domains, including the chloroplast transit peptide (TP, light gray), three chromodomains (CD1-3, dark gray), and four ankyrin repeats (Ank, light gray) are indicated. The position of the *Ds* transposon insertion in the *cpSRP43* gene in the *chaos* mutant is indicated. The primer recognition regions in *cpSRP43* are also shown. (*B*) PCR analyses of genomic DNA from the WT (Ler-0), *chaos*, and various *chaos* complementation lines confirmed the homozygosity of the *chaos* background, and revealed the different lengths of the amplicons generated from the WT and truncated *cpSRP43* coding sequences in various *chaos* complementation lines. To verify the expression of truncated cpSRP43 in *chaos* complementation lines, two primer pairs, pGL-cpSRP43-Fw + pGL-cpSRP43-Rev and pGL-cpSRP43ΔCD3-Rev, were employed. Furthermore, primer pair Ds3-4 + pGL-cpSRP43ΔCD3-Rev was used to confirm the *Ds* transposon insertion. (*C*) Schematic diagram of the *cpSRP43* gene showing the sites of the primer recognition regions used for qRT-PCR. (*D*) qRT-PCR analysis of *cpSRP43* gene expression in Ler-0, *chaos*, and various *chaos* complementation lines. *cpSRP43* expression is depicted relative to that in Ler-0, and normalized to *PEX4* (At5g25760). n.d., not detectable. *cpSRP43-#1* and *cpSRP43-#2* indicate the relative content of the transcripts derived from the respective *cpSRP43* genes when both qRT-PCR primer pairs (as shown in *C*) were applied. Data are means ± SD (n = 3).

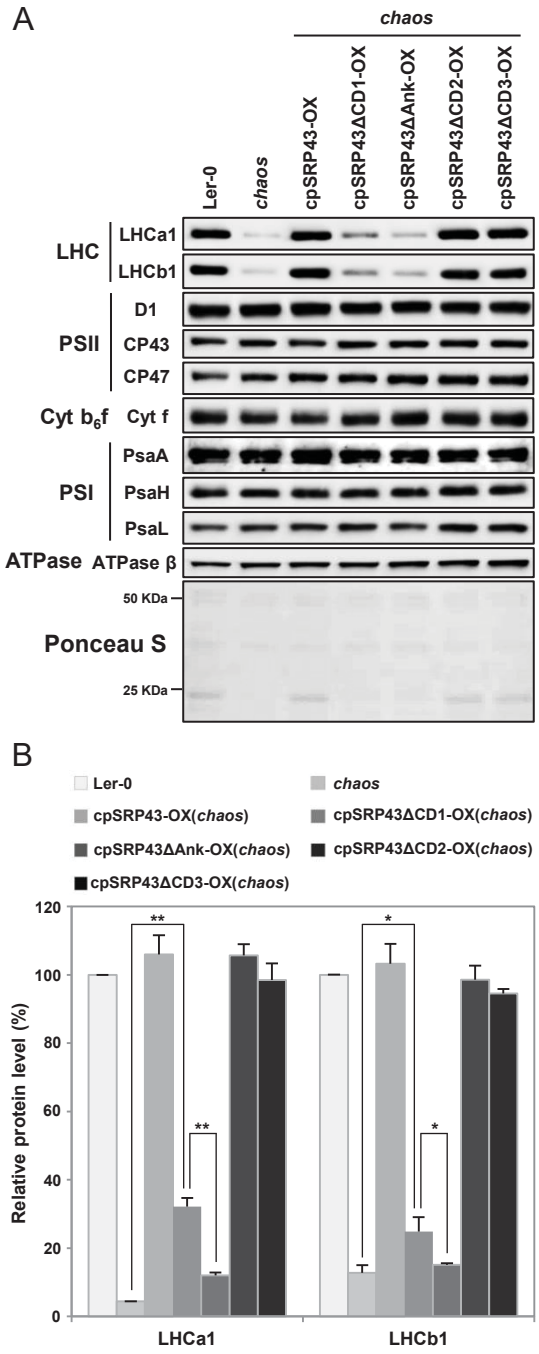

Fig. S7. Steady-state protein levels in the thylakoid membranes of Ler-0, *chaos* and various *chaos* complementation lines. (*A*) Aliquots (5 μg) of total thylakoid proteins were loaded on 11% SDS-urea-PA gels. Thylakoid membrane protein complexes and their diagnostic components are labeled on the left. The Ponceau S-stained nitrocellulose membrane is shown as a loading control. (*B*) Semiquantitative analyses of immunoblots in *A* from three biological replicates (see Fig. S1*D*). The relative amounts of thylakoid membrane proteins were normalized to the level of the β-subunit of the ATP synthase (ATPase β). The protein levels in *chaos* and *chaos* complementation lines are shown relative to those in Ler-0. Data are means ± SD (n = 3). Asterisks indicate significant differences compared with the wild-type plants (*P < 0.05, **P < 0.01, Student's t test).

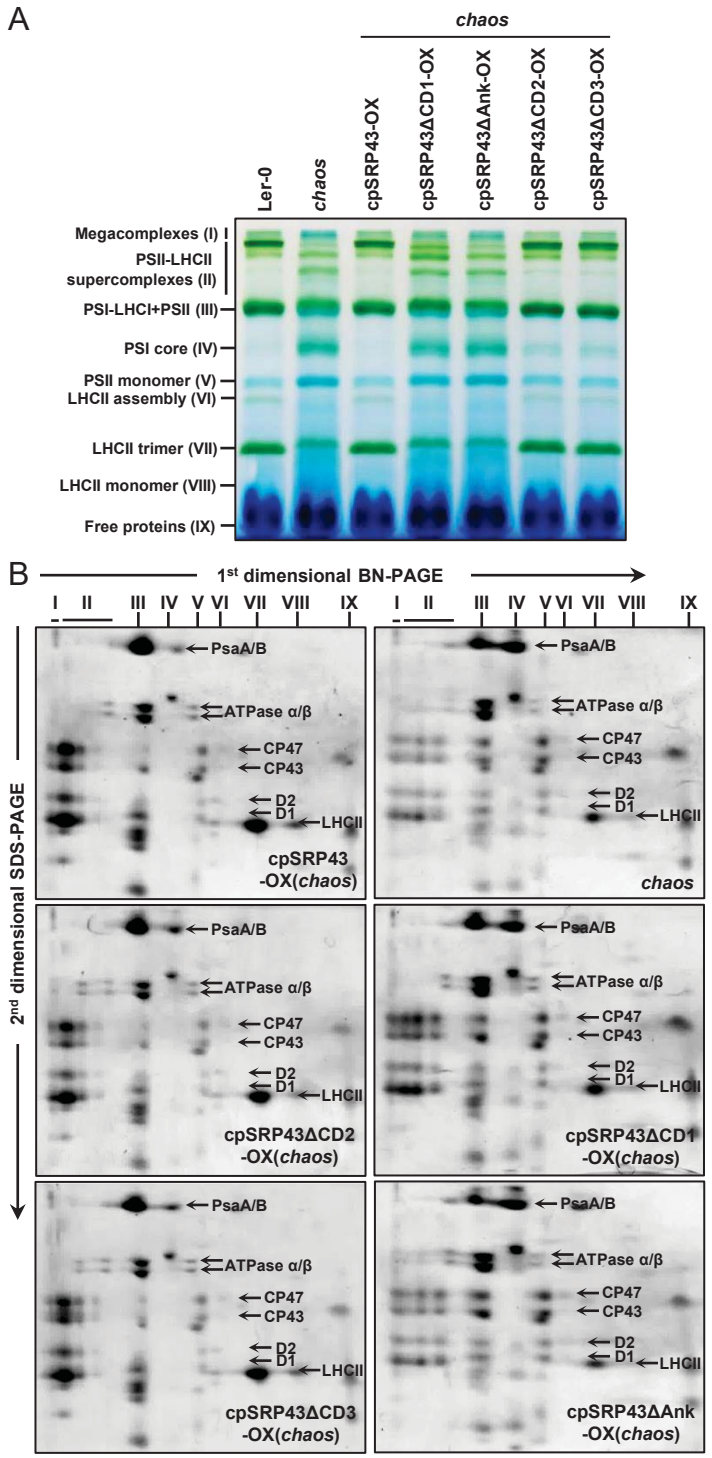

Fig. S8. Two-dimensional BN-SDS-PAGE analyses of thylakoid membrane pigment-protein complexes isolated from Ler-0, *chaos*, and various *chaos* complementation lines. (*A*) BN-PAGE analysis. Equal amounts of thylakoid membranes (8 μg of Chl) were solubilized with 1% (w/v) DM and fractionated on 4%-12% BN-PA gradient gels. (*B*) SDS-PAGE analysis. Individual lanes from the BN-PAGE gel in *A* were then subjected to 11% SDS-urea-PAGE. Total proteins were visualized by staining with Coomassie Brilliant Blue. Identities of the relevant proteins are indicated by arrows.

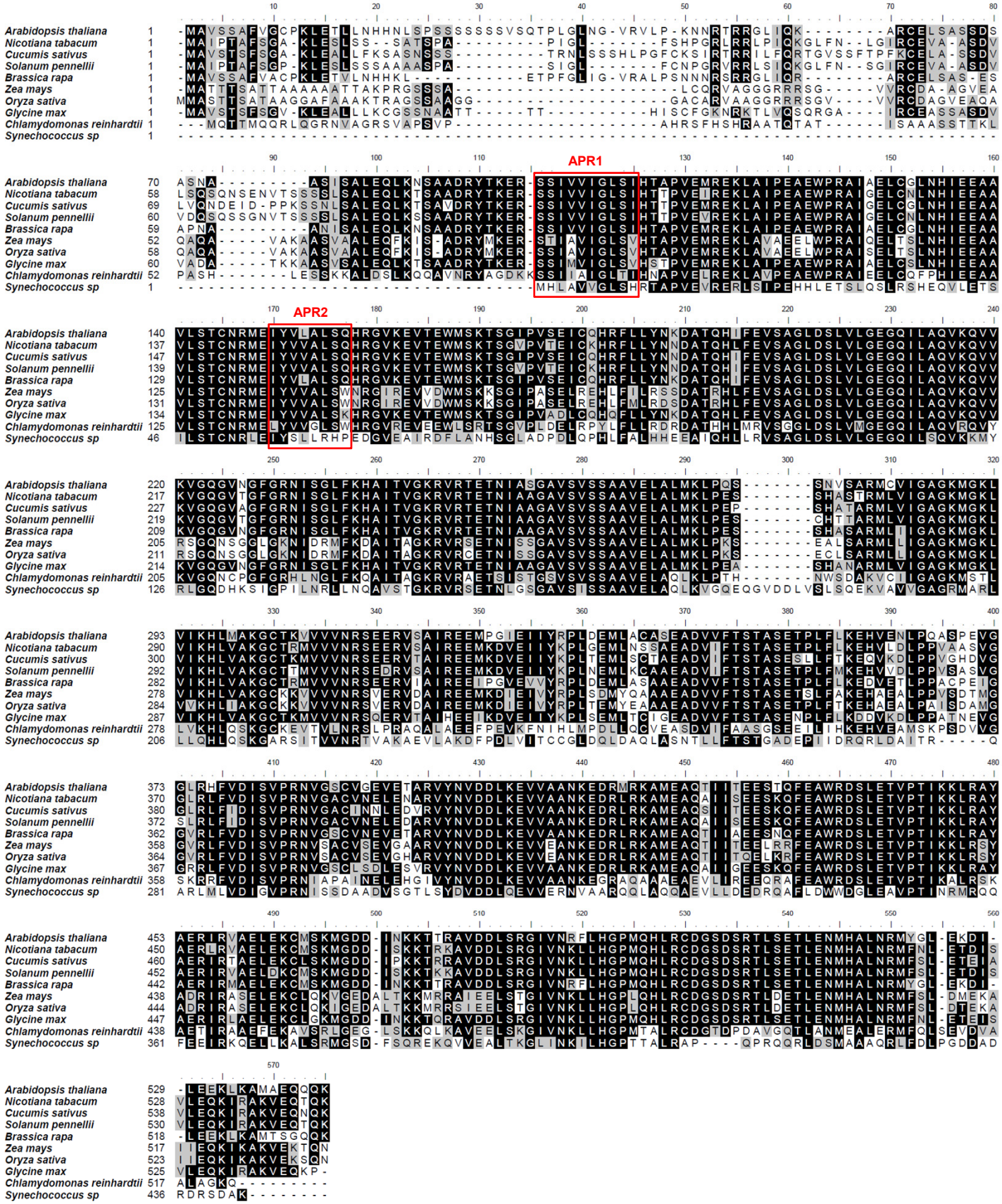

Fig. S9. Sequence alignment of *Arabidopsis* GluTR with homologs from different dicotelydons, *Chlamydomonas reinhardtii* and *Syncheocystis PCC sp 6803* by using ClustalW. Two APRs in GluTR are indicated by red frames.

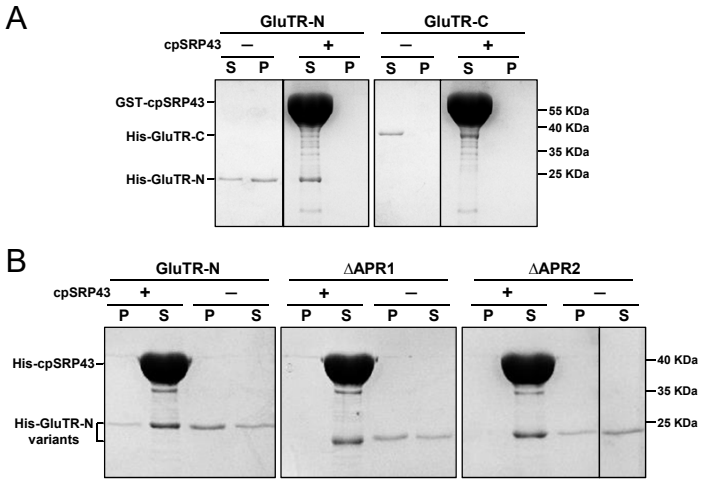

Fig. S10. Sedimentation assay indicates the capacity of cpSRP43 to prevent GluTR aggregation. (*A*) The solubility of N- and C-terminal parts of GluTR were compared with or without incubation with GST-cpSRP43. (*B*) The solubility of wild-type GluTR-N fragment and truncated GluTR-NΔAPR1 and GluITR-NΔAPR2 were compared with or without incubation with His-cpSRP43. P and S denote the pellet and soluble fractions, respectively. Proteins in P and S fractions were detected by staining with Coomassie Brilliant Blue.

Table S1: List of primers used in this study

qRT-PCR	Forward (Fw, 5'-3')	Reverse (Rev, 5'-3')
ACTIN2	CCGGTATTGTGCTCGATTCTG	TTCCCGTTCTGCGGTAGTGG
SAND	AACTCTATGCAGCATTTGATCCACT	TGATTGCATATCTTTATCGCCATC
cpSRP43-#1	CTGCACATGGCGGCTGGTT	CGTCTTTGCCTTTCCCTCGTT
cpSRP43-#2	TCTTCTGCTTTCTCCCCTGA	CGGCTTCCAATGATCTTGTT
HemA1	TTGCTGCCAACAAAGAAGAC	CCGTCTCCAATGAATCCCTC
GBP	CAGTTGACCGTGTTCTCC	AATCCAAGCCTATCCATC
FLU	AAGCCATACAGTATCACTCCA	TCCAGAATCTTCACTTTCCCT
GSAAT1	TCAAAGAAGAGCGACACAGAG	GTAAACACCTTCTTCCAACATTCC
CHLM	TTGCTGAAGCTGAGATGAAGGCA	CAACGGTATCATACTTCCCAGTTAG
CHL27	GCTTCTTCTGCCTCTCGGTTTATG	GCCGTGGTTCGGTTTGTCTCG
PORB	TGATTACCCTTCAAAGCGTCTCA	CAATGTATTCGTGTTCCCGGT
Plant transformation	Fw (5'-3')	Rev (5'-3')
pGL1-cpSRP43	TCTAGAATGCAAAAGGTCTTCTTGG	CCCGGGTCACTTGTCATCATCGTCCTTGTAGTCTTCATTCATTGG
pGL1-cpSRP43ΔCD3	TCTAGAATGCAAAAGGTCTTCTTGG	CCCGGGTCACTTGTCATCATCGTCCTTGTAGTCAGCGTACTCCAG
Intermediate primers for the cloning of truncated cpSRP43	Fw (5'-3')	Rev (5'-3')
cpSRP43ΔCD1	CATCATCATCGTACGCTAGAAAAGCCG	TCGGCTTTTCTAGCGTACGATGATGATG
cpSRP43ΔAnk	CCCTGGTGGACGGCACAAGTGTTCGAGTAC	GTACTCGAACACTTGTGCCGTCCACCAGG
cpSRP43ΔCD2	CAAGTGTTCGAGTACGTAGCGGAGAGTGT	GTACTCGAACACTTGTCCTTCCAGG
Genotyping	Fw (5'-3')	
Ds3-4	CCGTCCCGCAAGTTAAATATG	
BiFC constructs	Fw (5'-3')	Rev (5'-3')
pDonor-cpSRP43	CAAAAAAGCAGGCTGAATGCAAAAGGTCTTCTT	CAAGAAAGCTGGGTGTTCATTCATTGGTTGTTGT
pDonor-cpSRP54	CAAAAAAGCAGGCTGAATGGAGGCTCTTCAAT	CAAGAAAGCTGGGTGGTTACCAGAGCCGAAG
pDonor-cpFtsY	CAAAAAAGCAGGCTGAATGGCAACTTCTTCTGC	CAAGAAAGCTGGGTGAGAGAATATAGCATTCAC
pDonor-ALB3	CAAAAAAGCAGGCTGAATGGCGAGAGTTCTAGTCT	CAAGAAAGCTGGGTGTACAGTGCGTTTCCGCT
Prokaryotic expression constructs	Fw (5'-3')	Rev (5'-3')
pET28a-cpSRP43	GACATATGGCCGCCGTACAAAG	GCCTCGAGAGCGTACTCCAGCCCAT
pET28a-GluTR	ATCATATGGCTTCTTCTGATTCTGC	CTGAATTCTTACTTCTGTTGTTGTT
pET28a-GluTR-N	ATCATATGGCTTCTTCTGATTCTGC	CTCGAGTTATTATCGCGTGTTTAAA
pET28a-GluTR-C	ATCATATGCTGTTGGTAAGCGTGTT	CTGAATTCTTACTTCTGTTGTTGTT
ΔAPR1	ACAAAGGAAAGACACACAGCTCCT	AGGAGCTGTGTGTCTTTCCTTTGT
ΔAPR2	TAACCGTATGGAGCATCGTGGAGTT	AACTCCACGATGCTCCATACGGTT

References

1. Wang P & Grimm B (2016) Comparative Analysis of Light-Harvesting Antennae and State Transition in chlorina and cpSRP Mutants. *Plant Physiol* 172(3):1519-1531.
2. Apitz J, *et al.* (2016) Posttranslational Control of ALA Synthesis Includes GluTR Degradation by Clp Protease and Stabilization by GluTR-Binding Protein. *Plant Physiol* 170(4):2040-2051.
3. Apitz J, Schmied J, Lehmann MJ, Hedtke B, & Grimm B (2014) GluTR2 complements a hema1 mutant lacking glutamyl-tRNA reductase 1, but is differently regulated at the post-translational level. *Plant Cell Physiol* 55(3):645-657.
4. Edwards K, Johnstone C, & Thompson C (1991) A simple and rapid method for the preparation of plant genomic DNA for PCR analysis. *Nucleic Acids Res* 19(6):1349.
5. Kuromori T, *et al.* (2004) A collection of 11 800 single-copy Ds transposon insertion lines in Arabidopsis. *Plant J* 37(6):897-905.
6. Schlicke H, *et al.* (2014) Induced deactivation of genes encoding chlorophyll biosynthesis enzymes disentangles tetrapyrrole-mediated retrograde signaling. *Mol Plant* 7(7):1211-1227.
7. Mauzerall D & Granick S (1956) The occurrence and determination of delta-aminolevulinic acid and porphobilinogen in urine. *J Biol Chem* 219:435–446.
8. Walter M, *et al.* (2004) Visualization of protein interactions in living plant cells using bimolecular fluorescence complementation. *Plant J* 40(3):428-438.
9. Czarnecki O, *et al.* (2011) An Arabidopsis GluTR binding protein mediates spatial separation of 5-aminolevulinic acid synthesis in chloroplasts. *Plant Cell* 23(12):4476-4491.
10. Jaru-Ampornpan P, *et al.* (2010) ATP-independent reversal of a membrane protein aggregate by a chloroplast SRP subunit. *Nat Struct Mol Biol* 17(6):696-702.
11. Liu J, *et al.* (2012) PsbP-domain protein1, a nuclear-encoded thylakoid lumenal protein, is essential for photosystem I assembly in Arabidopsis. *Plant Cell* 24(12):4992-5006.
12. Chidgey JW, *et al.* (2014) A cyanobacterial chlorophyll synthase-HliD complex associates with the Ycf39 protein and the YidC/Alb3 insertase. *Plant Cell* 26(3):1267-1279.
13. Aronsson H & Jarvis P (2002) A simple method for isolating import-competent Arabidopsis chloroplasts. *FEBS Lett* 529(2-3):215-220.
14. Jarvi S, Suorsa M, Paakkarinen V, & Aro EM (2011) Optimized native gel systems for separation of thylakoid protein complexes: novel super- and mega-complexes. *Biochem J* 439(2):207-214.
15. Liang FC, *et al.* (2016) Conformational dynamics of a membrane protein chaperone enables spatially regulated substrate capture and release. *Proc Natl Acad Sci U S A* 113(12):E1615-1624.
16. Jaru-Ampornpan P, *et al.* (2013) Mechanism of an ATP-independent protein disaggregase: II. distinct molecular interactions drive multiple steps during aggregate disassembly. *J Biol Chem* 288(19):13431-13445.